Clim Dyn (2013) 40:551–568
DOI 10.1007/s00382-012-1605-8

Mid-twenty-first century warm season climate change in the Central United States. Part I: regional and global model predictions

Christina M. Patricola · Kerry H. Cook

Received: 21 June 2011 / Accepted: 17 November 2012 / Published online: 13 December 2012

Abstract A regional climate model (RCM) constrained by future anomalies averaged from atmosphere–ocean general circulation model (AOGCM) simulations is used to generate mid-twenty-first century climate change predictions at 30-km resolution over the central U.S. The predictions are compared with those from 15 AOGCM and 7 RCM dynamic downscaling simulations to identify common climate change signals. There is strong agreement among the multi-model ensemble in predicting wetter conditions in April and May over the northern Great Plains and drier conditions over the southern Great Plains in June through August for the mid-twenty-first century. Projected changes in extreme daily precipitation are statistically significant over only a limited portion of the central U.S. in the RCM constrained with future anomalies. Projected changes in monthly mean 2-m air temperature are generally consistent across the AOGCM ensemble average, North American Regional Climate Change Assessment Program RCM ensemble average, and RCM constrained with future anomalies, which produce a maximum increase in August of 2.4–2.9 K over the northern and southern Great Plains and Midwest. Changes in extremes in daily 2-m air temperature from the RCM downscaled with anomalies are statistically significant over nearly the entire Great Plains and Midwest and indicate a positive shift in the warm tail of the daily 2-m temperature distribution that is larger than the positive shift in the cold tail.

Keywords Regional climate model · Climate change · Central United States · Great Plains · Midwest · Precipitation · Model intercomparison · NARCCAP · Downscaling

C. M. Patricola
Department of Earth and Atmospheric Sciences, Cornell University, Ithaca, NY 14853, USA

C. M. Patricola (✉)
Department of Atmospheric Sciences, Texas A&M University, 3150 TAMU, College Station, TX 77843-3150, USA
e-mail: cmd58@cornell.edu

K. H. Cook
Jackson School of Geosciences, The University of Texas at Austin, 1 University Station, C1100, Austin, TX 78712, USA

1 Introduction

Mid-twenty-first century climate prediction on the regional scale is needed to better understand and plan for climate change impacts in the central United States (including IA, IL, IN, KS, western KY, western MN, MO, ND, NE, OK, SD, and northern TX). The coupled atmosphere–ocean general circulation models (AOGCMs) run for the Fourth Assessment Report of the Intergovernmental Panel on Climate Change (IPCC AR4; IPCC 2007) provide information about future climate on spatial scales of about 200 km, and the Climate Model Intercomparison Project 5 (CMIP5) integrations run for the Fifth Assessment Report generally increase this resolution to about 100 km. Regional climate models (RCMs) can bring this resolution to a few tens of kilometers, and dynamic downscaling with RCMs may offer predictions with reduced climate bias compared to global model simulations (e.g., Liang et al. 2008). Even though regional models use dynamical cores and physical parameterizations similar to those used in general circulation models (GCMs), the ability to optimize simulations for one region can produce a marked improvement in the simulation of present day climate, which could increase (but not guarantee) confidence in future projections.

The purpose of this work is to synthesize climate change projections over the central U.S. for 2041–2060, with a focus on monthly climatologies and daily extremes of warm season precipitation and 2-m air temperature, from an ensemble of 15 AOGCMs of the IPCC AR4, 7 RCM simulations from the North American Regional Climate Change Assessment Program (NARCCAP; Mearns et al. 2009), and a RCM simulation run for this study that uses higher resolution and an alternative downscaling technique that reduces climate bias in the present day simulation.

We focus on predicted changes in central U.S. warm season precipitation and 2-m air temperature since variability in these quantities can have significant socioeconomic and agricultural impacts. For example, the 1988 central U.S. drought and heat wave, which brought precipitation deficits comparable to those of the 1930 s "Dust Bowl" (Kunkel and Angel 1989), resulted in ~\$40 billion in losses and over 5,000 deaths (Lott and Ross 2006). Flooding in the central U.S. also takes a heavy toll on life, agriculture, property, infrastructure, and the economy [e.g., the summer 1993 Midwest flood caused \$21 billion in damage and 48 fatalities (Lott and Ross 2006)]. Dynamically downscaled RCM simulations suggest an increase in the frequency of late twenty-first century central U.S. drought and flood events (Bukovsky and Karoly 2011); regional scale predictions such as this can help policy makers plan for the impacts of climate change.

The next section provides a brief discussion of climate change prediction methodologies along with details about the alternative downscaling technique and its advantages and disadvantages. The RCM simulation design is presented in Sect. 3, and Sect. 4 includes a validation of the warm season monthly mean and diurnal cycle of central U.S. precipitation. Mid-twenty-first century climate change projections of monthly mean warm season precipitation and 2-m air temperature from the AOGCM and RCM ensembles and the RCM that is downscaled with anomalies are in Sect. 5, along with projected changes in measures of extreme daily precipitation and 2-m air temperature from the RCM downscaled with anomalies. Conclusions are in Sect. 6. The aim of examining an alternate downscaling technique alongside multi-model ensembles in this study is to strengthen confidence in the projected climate changes. To further our understanding of the confidence that can be placed in the precipitation changes projected by the RCM downscaled with anomalies, connections between precipitation and circulation changes, including the Great Plains low-level jet, are analyzed in Part II (Patricola and Cook 2012).

2 Methods of climate change prediction

Modeling choices for past, present, and future climate simulations depend on the time scales and regions of interest. For studies of large-scale climate change on time scales of centuries and greater, it is often advantageous to use AOGCMs since large-scale teleconnections and climate feedbacks are explicitly simulated, and since integration length may be gained at the expense of spatial resolution. The use of RCMs for projecting future climate change has been gaining popularity as the demand for high-resolution predictions increases. The regional model allows finer resolution to be gained at the expense of spatial coverage, however use of the RCM introduces the need for a data/model source to prescribe lateral boundary conditions (LBCs) and, in atmosphere-only RCMs, sea surface temperature (SST). Several studies find that LBCs generate a large source of uncertainty in RCM simulations, which can arise from random perturbations in LBCs (Giorgi and Bi 2000), using different reanalysis products to prescribe LBCs (Gong and Wang 2000), and varying the frequency at which LBCs update and the spatial resolution of LBCs (Dimitrijevic and Laprise 2005; Diaconescu et al. 2007). The uncertainties generated in a RCM by uncertainties in LBCs can exceed those due to varying initial condition, model resolution, physical parameterization, and RCM used (Vukicevic and Errico 1990; de Elía et al. 2008; Arritt and Rummukainen 2011). Interactions of the synoptic flow generated by the RCM with the prescribed outflow along lateral boundaries can result in inconsistencies near RCM domain edges and also produce biases in the simulations; spectral nudging of the long waves in RCM simulations with domains extending 1,000 s of km or larger markedly improves the simulation of the small scale circulation and precipitation over the U.S. in summer when the large scale circulation imposed in the LBCs is relatively weak compared to internal forcings in the model (Miguez-Macho et al. 2004).

The traditional approach to prescribing boundary conditions for climate change studies using a RCM, referred to as dynamic downscaling, is to impose LBCs and SST directly from an AOGCM for both the control and future integrations. The regional model simulations of NARCCAP use dynamic downscaling to produce a multi-model set of 50-km resolution climate change simulations for the mid-twenty-first century forced by the SRES A2 emissions scenario over North America. The NARCCAP simulations use various combinations of RCMs and AOGCMs (Table 1). Dynamic downscaling prescribes the synoptic and large-scale circulation of AOGCMs, including teleconnections and interannual variability, through the LBCs. However, one drawback of the dynamic downscaling approach is that biases from the AOGCM that provides LBCs and SST are introduced into the RCM, which can degrade the representation of present day (and future) climate. For example, the simulation of present day climatological South American precipitation and vegetation

Table 1 NARCCAP simulations (Mearns et al. 2009)

Simulation name	Regional model	AOGCM providing boundary conditions
NARCCAP_1	Canadian Regional Climate Model (CRCM)	Canadian Climate Centre CCCMA_CGCM3.1
NARCCAP_2	Met Office Hadley Centre's Hadley Regional Model 3 (HadRM3)	Hadley Centre UKMO-HadCM3
NARCCAP_3	Abdus Salam International Center for Theoretical Physics Regional Climate Model Version 3 (RegCM3)	Canadian Climate Centre CCCMA_CGCM3.1
NARCCAP_4	Abdus Salam International Center for Theoretical Physics Regional Climate Model Version 3 (RegCM3)	Geophysical Fluid Dynamics Laboratory GFDL-CM2.1
NARCCAP_5	National Center for Atmospheric Research Weather Research and Forecasting Model (WRF)	National Center for Atmospheric Research NCAR_CCSM3
NARCCAP_6	Canadian Regional Climate Model (CRCM)	National Center for Atmospheric Research NCAR_CCSM3
NARCCAP_7	NCAR/Pennsylvania State University Mesoscale Model 5 (MM5)	National Center for Atmospheric Research NCAR_CCSM3

suffered large biases when LBCs were prescribed from a GCM, while the biases were minimal when LBCs were prescribed from reanalysis (Cook and Vizy 2008).

Several approaches can be taken in evaluating climate change prediction with RCM or GCM simulations. One possibility is to select models based on validation of the present day simulation, with focus on the variables of interest and circulation features that play an important role in the variables of interest. For example, by analyzing a subset of AOGCMs selected according to their simulation of the warm season Great Plains low-level jet (GPLLJ) and precipitation, a consensus in late twenty-first century projections emerges with increased precipitation in the upper Mississippi Valley and a stronger GPLLJ during spring (Cook et al. 2008). Another approach involves considering all simulations, regardless of bias, with the assumption that a bias in the present day simulation will also exist in the future simulation, and so will cancel in the difference as supported by Liang et al. (2008).

However, while it is possible that similar biases may exist in present day and future simulations from both RCMs and AOGCMs, a negative bias in variables that have a lower limit of zero, like precipitation, adds uncertainty to future projections. That is, a model with a severe dry precipitation bias cannot project future drying. Another likely source of uncertainty in dynamically downscaled RCM simulations in the Atlantic region can arise from prescribing SST from AOGCMs, which commonly suffer a severe eastern equatorial Atlantic warm SST bias during boreal summer (Davey et al. 2002; Richter and Xie 2008). That bias is particularly problematic because many atmospheric phenomena, including the West African monsoon system (e.g., Lamb 1978; Bah 1987; Vizy and Cook 2001 and references therein) and Atlantic tropical cyclones, are sensitive to eastern equatorial Atlantic SST.

Motivated by the problem of increased uncertainty in future climate projections due to biased current climate simulations, we employ an alternative technique for projecting future climate with RCMs, which we call downscaling with anomalies. This approach prescribes SST and LBCs from reanalysis for the present day simulation, with the benefit that AOGCM biases are not carried into the RCM. For the future simulation, future anomalies projected by AOGCMs are added to the reanalysis to create the LBCs and SST for the RCM. Here, the future anomalies are taken from an ensemble average of six AOGCMs; using an ensemble average, rather than an individual AOGCM, may reduce uncertainty in the future LBCs, as Yang et al. (2011) find that biases in four RCM simulations driven by LBCs from four different reanalysis products are somewhat reduced by using the equally-weighted average of the four reanalysis products as LBCs, and are greatly reduced by using the Bayesian model averaging ensemble mean of the four reanalysis products as LBCs. The downscaling with anomalies method accounts for future changes in the mean state of the atmosphere and ocean from the AOGCM simulation. However a disadvantage is that future changes in transients and interannual variability from the AOGCM are not included in the LBCs and SST, and are prescribed to be identical to the present day simulation.

In this paper we analyze simulations that use the various methods of climate change projections described above, including a 15-member ensemble of AOGCMs from the IPCC AR4, a 7-member ensemble of NARCCAP dynamically downscaled RCMs, and the RCM that is downscaled with anomalies and is described in the next section.

3 Methodology

Regional climate model simulations are conducted with the Weather Research and Forecasting Model (WRF; Skamarock et al. 2008) version 3.1. WRF is a non-hydrostatic model configured with 30 vertical levels and the top of the atmosphere set to 30 hPa (with 8 half-sigma levels below 850 hPa, 6 between 850 and 500 hPa, 8 between 500 and 150 hPa, and 7 between 150 and 30 hPa over regions with topography height close to zero). Monthly-varying albedo, fractional sea ice, and gravity wave drag are used. Physical parameterizations (described in Skamarock et al. 2008 and references therein) include the Lin microphysics, CAM longwave and shortwave radiation, Monin–Obukhov surface layer scheme, Yonsei University (YSU) planetary boundary layer, Kain-Fritsch cumulus scheme, and the Noah land-surface model.

The RCM uses two-way nested 90 and 30-km domains. The parent domain (Fig. 1a), which has 90-km resolution and a 6-min time step, includes the North Atlantic Ocean and subtropical high. We choose 90-km resolution to represent the subtropical high since it is a large-scale feature that strongly influences the warm season climate in the central U.S., and place the eastern boundary to allow the entire high to exist within the domain. The inner domain (Fig. 1b) uses 30-km horizontal resolution and a 2-min time step. The fine resolution better resolves the Great Plains low-level jet and topography compared to coarser resolution models (e.g., Fig. 2 of Cook et al. 2008), and provides information suitable for impacts analysis in the central U.S. Analysis regions (Fig. 1b), including the "northern Great Plains," "southern Great Plains," and "Midwest," are chosen based on the simulated present day warm season precipitation climatology, and to cover areas of the same sign of future monthly precipitation predictions (presented in Sect. 5a).

The late-twentieth century simulation, named "L20," consists of twenty individual annual simulations for 1981–2000. The RCM is first initialized on 1 January 1980 using soil moisture and temperature from the 32-km North American Regional Reanalysis (NARR; Mesinger et al. 2006) 1980–2000 January average, and run through 1 December 1980. The simulation of 1 January 1980 to 1 December 1980 is disregarded for model spin up. The first annual simulation is then initialized on 1 December 1980 and run through 31 December 1981, with the first month disregarded for spin-up. Each of the twenty annual integrations for L20 is formed this way. At the start of each annual integration, the atmospheric variables are initialized from reanalysis products, while the surface temperature, snow cover, and soil moisture and temperature are initialized from the previous model integration. Model output is saved every 3 h.

Lateral boundary conditions for L20 are prescribed from the 6-hourly 2.5° × 2.5° National Centers for Environmental Prediction/Department of Energy Atmospheric Model Intercomparison Project II (NCEP/DOE AMIP-II) Reanalysis (Kanamitsu et al. 2002). The European Centre for Medium-Range Weather Forecasts (ECMWF 2002) reanalysis is used to prescribe initial snow cover and monthly averaged SSTs since its resolution (~1.4° × ~1.4°) is finer than that of NCEP-II (~1.9° × ~1.9°). Fractional sea ice is prescribed according to the monthly NCEP/NCAR reanalysis (Kalnay et al. 1996), which is relatively similar to NCEP-II for our region and period of interest. Monthly SST and sea ice are used since the high frequency variability of SST and sea

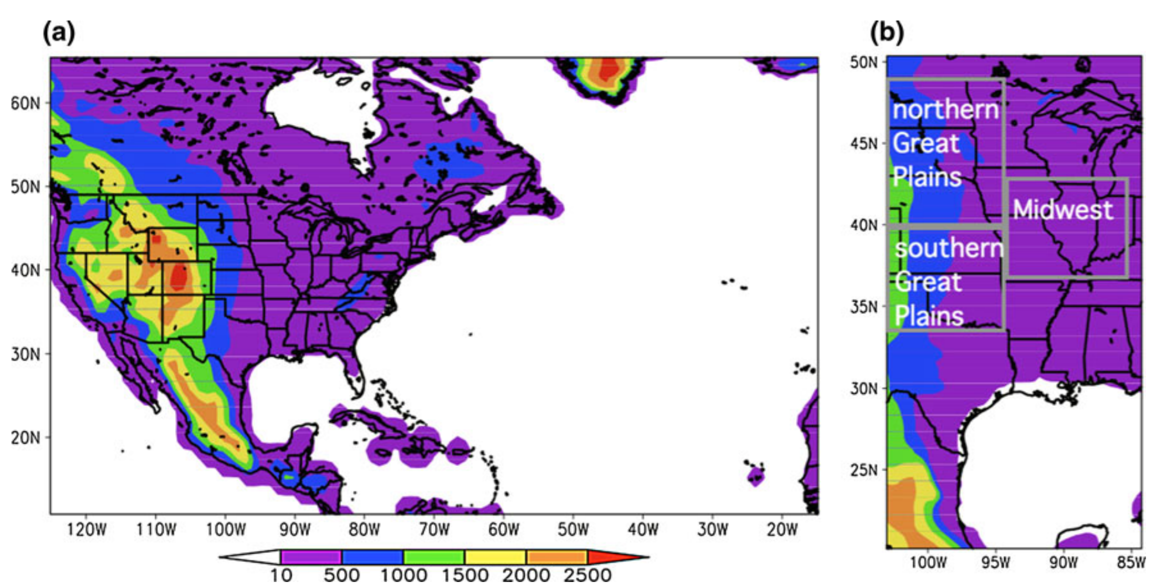

Fig. 1 Topography (m) at **a** 90-km resolution on the parent domain and **b** 30-km resolution on the inner domain with averaging regions including the northern Great Plains (40.1°N–48.9°N, 103.0°W–94.3°W), southern Great Plains (33.8°N–39.8°N, 103.0°W–94.3°W), and Midwest (36.8°N–42.3°N, 94.0°W–85.0°W) shown in *grey boxes*

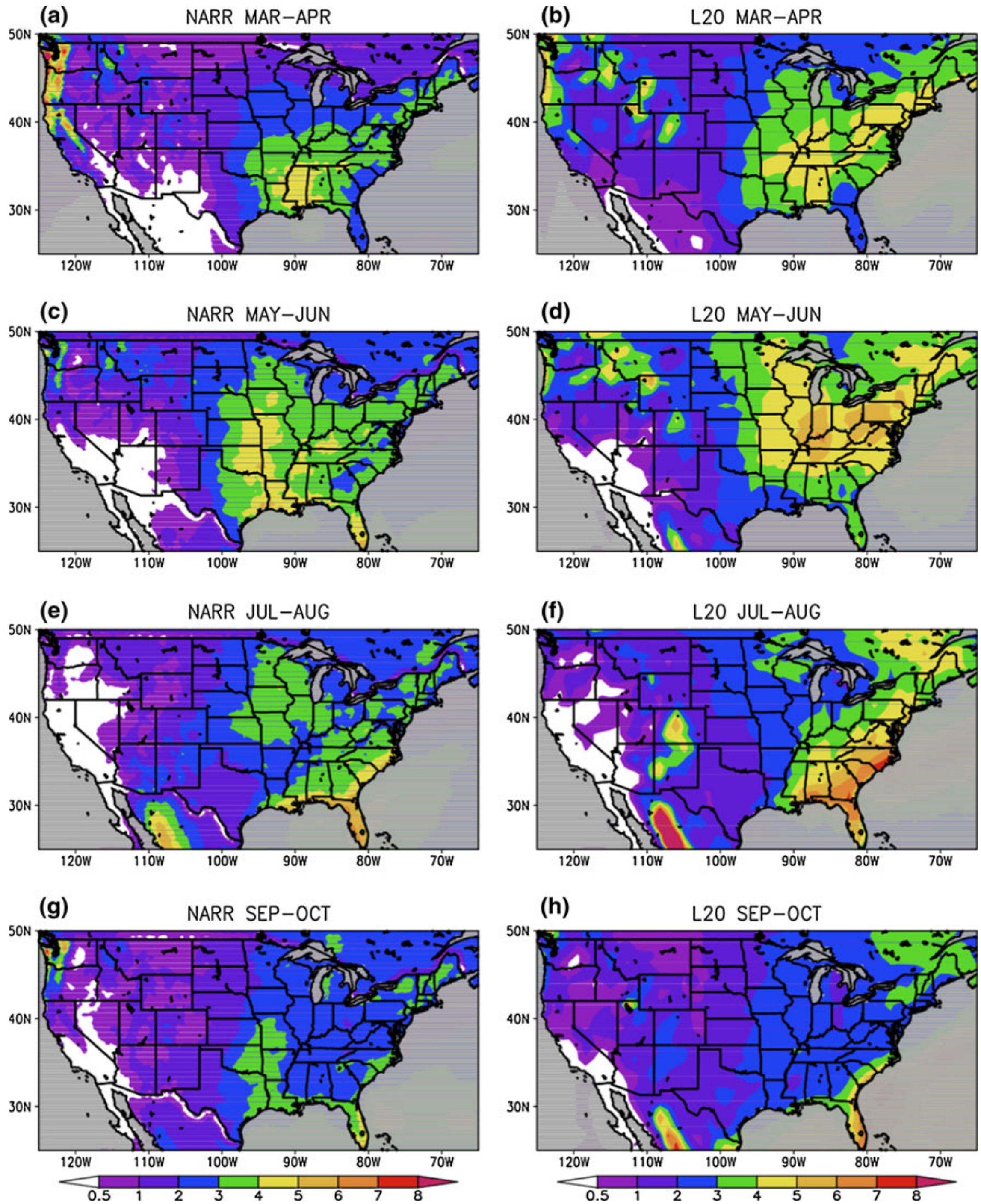

Fig. 2 Precipitation rate (mm/day) averaged **a**, **b** March–April, **c**, **d** May–June, **e**, **f** July–August, and **g**, **h** September–October of 1981–2000 from NARR and the 90-km domain of the L20 simulation, respectively. Values over water are masked *grey*

ice is not essential to this study. The RCM updates boundary conditions every 6 h.

The future climate simulation, “M21,” represents 2041–2060 and consists of twenty annual integrations that are spun-up and initialized in the same way as L20. Atmospheric CO_2, N_2O, CH_4, CFC-11, and CFC-12 concentrations are prescribed based on the SRES A2 emissions scenario (IPCC 2000), which estimates high greenhouse gas emissions relative to other scenarios in association with high population growth and slow diffusion of technological change. The CO_2 concentration updates annually, from 339.6 to 370.5 ppm in L20, and 533.0 to 578.0 ppm in M21. N_2O, CH_4, CFC-11, and CFC-12 concentrations are prescribed at the 20-year average and are modified from

0.311 ppm, 1.714 ppm, 0.280 ppb, and 0.503 ppb, respectively, in L20 to 0.373 ppm, 2.562 ppm, 0.123 ppb, and 0.362 ppb, respectively, in M21.

LBCs and SSTs for the future simulations are applied as anomalies generated from the ensemble average of monthly climatologies of six AOGCM simulations (denoted in Table 2), similar to the method used by Patricola and Cook (2010). Schneider et al. (2009) prescribe SSTs in a similar way in simulations with the NCAR Community Atmosphere Model, by using observed monthly SSTs for current-era climate simulations and adding monthly anomalies in decadal means (2065–2075 minus 1965–1975) from a single AOGCM and an ensemble average of 15 AOGCMs to the observed monthly SST to construct future SST. The six AOGCMs used in this study were chosen because they reasonably well represent the present day Great Plains low-level jet (see Cook et al. 2008), which plays an important role in central U.S. warm season precipitation variability (e.g., Mo et al. 1997; Weaver and Nigam 2008), and because the future (2041–2060 minus 1981–2000) SST projections are generally consistent among the models, with cooling or a minimum in warming in the north Atlantic Ocean south of Greenland. The AOGCM anomalies are the 2041–2060 monthly average forced by the SRES A2 emissions scenario minus the simulated 1981–2000 monthly average.

In creating the future LBCs, the ensemble average of monthly climatological anomalies of six AOGCM simulations are interpolated to 6-hourly intervals on the reanalysis grid and added to the 6-hourly fields of the NCEP II reanalysis used in L20. For example, LBCs for L20 on 00z 15 June 1981 are taken from the NCEP II reanalysis on 00z 15 June 1981. Then, LBCs for the M21 simulation on 00z 15 June 2041 are calculated by adding the reanalysis on 00z 15 June 1981 to the AOGCM climatological monthly ensemble average of June 2041–2060 minus the AOGCM climatological monthly ensemble average of June 1981–2000. Therefore, the future LBCs account for changes in the mean climate state, but do not include changes in transients or interannual variability. This does not imply that transients generated by the RCM within the domain are the same between L20 and M21. Since the transients and interannual conditions of 1981 are obviously not expected to occur in 2041, we analyze the 20 years of M21 not as representing a specific year, but consider the 20 years together as representing the 2040 and 2050 decades.

Future SSTs and sea ice are also derived from the monthly climatological ensemble average of the six AOGCM simulations, interpolated to the reanalysis grid,

Table 2 IPCC AR4[a] simulations analyzed in this study (see Table 8.1 in IPCC (2007) for details)

Short name	AOGCM	Sponsor(s), Country
CCCMA[b]	CCCMA_CGCM3.1	Canadian Centre for Climate Modelling and Analysis, Canada
CNRM[b]	CNRM-CM3	Météo-France/Centre National de Recherches Météorologiques, France
CSIRO	CSIRO_Mk3.0	Commonwealth Scientific and Industrial Research Organisation (CSIRO) Atmospheric Research, Australia
ECHO	MIUB_ECHO_G	Meteorological Institute of the University of Bonn, Meteorological Research Institute of the Korea Meteorological Administration (KMA), and Model and Data Group, Germany/Korea
GFDL_0[b]	GFDL-CM2.0	U.S. Department of Commerce/National Oceanic and Atmospheric Administration (NOAA)/ Geophysical Fluid Dynamics Laboratory (GFDL), USA
GFDL_1	GFDL-CM2.1	U.S. Department of Commerce/National Oceanic and Atmospheric Administration (NOAA)/ Geophysical Fluid Dynamics Laboratory (GFDL), USA
GISS_ER	GISS_ER	National Aeronautics and Space Administration (NASA)/Goddard Institute for Space Studies (GISS), USA
INMCM	INM-CM3.0	Institute for Numerical Mathematics, Russia
IPSL	IPSL-CM4	Institut Pierre Simon Laplace, France
MIROC_MED	MIROC3.2 (medres)	Center for Climate System Research (University of Tokyo), National Institute for Environmental Studies, and Frontier Research Center for Global Change (JAMSTEC), Japan
ECHAM5[b]	ECHAM5/MPI-OM	Max Planck Institute for Meteorology, Germany
MRI	MRI-CGCM2.3.2	Meteorological Research Institute, Japan
CCSM	NCAR_CCSM3	National Center for Atmospheric Research, USA
PCM[b]	NCAR_PCM	National Center for Atmospheric Research, USA
HADCM[b]	UKMO-HadCM3	Hadley Centre for Climate Prediction and Research/Met Office, UK

[a] AOGCM output is from the World Climate Research Programme's (WCRP's) Coupled Model Intercomparison Project phase 3 (CMIP3) multi-model dataset (Meehl et al. 2007), archived by the Program for Climate Model Diagnosis and Intercomparison

[b] Simulations used to create boundary conditions for the M21 simulation

and applied as anomalies to the monthly values from the reanalyses.

4 Warm season precipitation and RCM validation

The ability of the RCM to represent observed climate is assessed to support confidence in the future projections, recognizing that a good simulation of the late twentieth century does not guarantee accurate prediction for the twenty-first century. The observed characteristics of warm season precipitation in the central U.S. are presented and compared with monthly precipitation of late twentieth century simulations from the ensemble of AOGCMs, the ensemble of NARCCAP RCMs, and the RCM downscaled with anomalies. We also validate the diurnal cycle of warm season precipitation of L20 and an AOGCM since this helps demonstrate whether a model is likely representing the physical processes associated with precipitation that occur in nature, and so can provide additional insight into uncertainty or support of future projections.

Figure 2 shows precipitation rates averaged March–April, May–June, July–August, and September–October of 1981–2000 from the assimilated precipitation of the NARR (Mesinger et al. 2006) and the 90-km domain of L20 over the continental U.S. The averaging periods of MA, MJ, JA, and SO are chosen because the precipitation climatology of the individual months is similar in each pair. We focus on the warm season to support the analysis of future projections in Sect. 5a, but note that the spatial distribution and magnitudes of monthly precipitation during the cold season from L20 compare very well with NARR (not shown). In NARR there is a maximum of 4–5 mm/day centered over Mississippi and Alabama in March–April (Fig. 2a), and in May–June the maximum spreads northward over Kansas, Missouri, and Oklahoma (Fig. 2c). The RCM captures the northwestward shift, although the maximum is displaced to the east and is stronger in the RCM (Fig. 2b, d). The central U.S. precipitation maximum advances north in July–August with rates of 3–4 mm/day (Fig. 2e). The RCM (Fig. 2f) reproduces this, but with modeled precipitation rates over the northern Great Plains and southeastern U.S. that are weaker and stronger than assimilated, respectively (Fig. 2e). In September–October, the rainfall maximum retreats south in both the NARR and L20 (Fig. 2g, h).

Next we compare the assimilated precipitation averaged from July and August of 1981–2000 (Fig. 2e), with that of 15 AOGCMs (Fig. 3; Table 2). All AOGCMs that were available at the time of this analysis were used. We considered precipitation during both the May–June and the July–August averaging periods and find results are relatively insensitive to which group of months is chosen to represent the warm season, so for conciseness we present results for July and August only. Only three AOGCMs (Fig. 3a–c) generally reproduce the magnitude and location of the central precipitation maximum and the zonal rainfall gradient to the west (compare with Fig. 2e). Five models (Fig. 3d–h) simulate unrealistically heavy rainfall centered near northeastern Colorado, while another common bias is too little rainfall in the central U.S. (Fig. 3i–n). Another model (Fig. 3o) produces too much precipitation over western Texas, Oklahoma, and Nebraska.

We also validate precipitation averaged from July and August of 1981–2000 from seven NARCCAP RCM simulations that use AOGCM boundary conditions (Fig. 4; Table 1). Some simulations (compare with Fig. 2e) are too dry over the central U.S. (Fig. 4a, e, f) or Florida (Fig. 4g), while others simulate a westward bias in rainfall (Fig. 4c, d) similar to many AOGCMs (Fig. 3d–h). One simulation (Fig. 4b) produces an eastward bias in the central U.S. precipitation maximum similar to L20 (Fig. 2f). As expected since it is driven with reanalysis, the simulated monthly climatological precipitation of L20 (Fig. 2f) matches better with observations (Fig. 2e) than most AOGCM simulations (Fig. 3) and is comparable to or better than the NARCCAP simulations (Fig. 4).

A validation of the diurnal warm season central U.S. precipitation cycle, which is characterized by a strong nocturnal peak as shown by the 0.25° × 0.25° Tropical Rainfall Measuring Mission (TRMM) 3B43 Version 6 satellite data (Huffman et al. 2007) and NARR (Fig. 5), reveals whether or not a model is likely representing the processes that produce rainfall and so can help assess confidence or uncertainty in a model. Radar data (Carbone and Tuttle 2008) and hourly rain gauge data (Chen et al. 2009) support the secondary late afternoon rainfall maximum of NARR and TRMM over the Midwest (Fig. 5b).

Realistic simulation of the observed warm season diurnal rainfall cycle over the central U.S. is challenging. Models often do not capture the nocturnal maximum, and instead produce a single afternoon maximum (e.g., Lee et al. 2007), with no significant improvement achieved by increasing model resolution up to 50-km (Lee et al. 2008). Liang et al. (2004, 2006) find that the diurnal rainfall cycle in present day and future simulations is strongly dependent on the convective parameterization. This is supported by Han and Roads (2004), who suggest that differences between warm season central U.S. precipitation simulated by a global model and a dynamically-downscaled RCM are largely related to differences in convective parameterizations.

The diurnal cycle of rainfall averaged June–August from L20 and a twentieth century simulation of the GFDL_CM2.0 AOGCM, which is chosen as an example to demonstrate the common diurnal rainfall bias, is compared

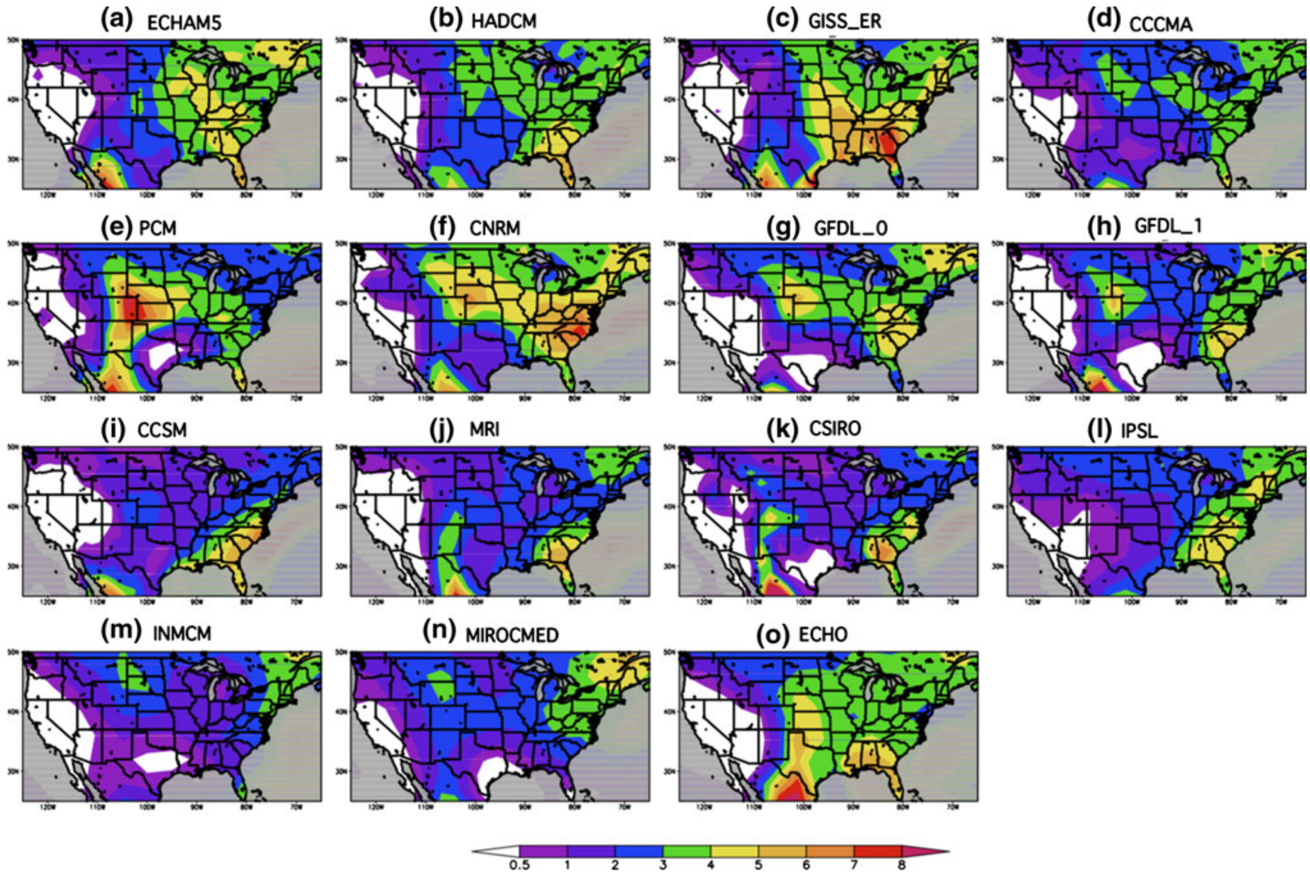

Fig. 3 Precipitation rate (mm/day) averaged July–August of 1981–2000 from 15 AOGCM simulations. Values over water are masked *grey*. Refer to Fig. 2e for observed precipitation. **a** ECHAM5, **b** HADCM, **c** GISS_ER, **d** CCCMA, **e** PCM, **f** CNRM, **g** GFDL_0, **h** GFDL_1, **i** CCSM, **j** MRI, **k** CSIRO, **l** IPSL, **m** INMCM, **n** MIROCMED, **o** ECHO

with NARR and TRMM (Fig. 5). The northern and southern Great Plains are plotted together in Fig. 5a since the observed and simulated diurnal cycles are similar over the two individual regions. JJA rainfall in NARR and TRMM peaks at 0000 LT over the Great Plains (Fig. 5a), while there is a dual peak, the greater at 0300 LT and the smaller at 1800 LT, in both rainfall products over the Midwest (Fig. 5b). Similar to the TRMM and NARR, L20 simulates the two Midwest maxima, although the 1800 LT maximum is unrealistically stronger than the 0300–0600 LT maximum (Fig. 5b). The dual maximum in L20 suggests that the RCM is capturing both the afternoon and nighttime rainfall processes, although the afternoon rainfall is overrepresented. The RCM also simulates a dual peak in diurnal rainfall over the Great Plains that does not represent the observations well (Fig. 5a). However, over both regions the RCM is a marked improvement over the AOGCM, which simulates one rainfall maximum at 1200–1500 LT and produces a minimum overnight. While the RCM more closely represents the observed diurnal rainfall cycle compared to some, but not all, AOGCM simulations (Lee et al. 2007), there remains room for improvement in the RCM with respect to this common modeling challenge.

5 Mid-twenty-first century predictions

5.1 Monthly mean precipitation

Projected changes in monthly averaged warm season precipitation for the mid-twenty-first century from M21–L20 are shown in Fig. 6. Conditions are predicted to be generally wetter in April and May (Fig. 6, b) and drier during July and August (Fig. 6d, e) over the Great Plains and Midwest. In June (Fig. 6c) wetter and drier conditions are predicted over the northern and southern Great Plains respectively, with the opposite in September (Fig. 6f). Based on these projected changes, we consider the absolute (Fig. 7a) and relative (Fig. 7b) monthly precipitation projections of M21–L20 over the three averaging regions from Fig. 1b in order to isolate the simulated climate change signals and quantify their relative change. Although projected changes are shown for the entire year we focus on

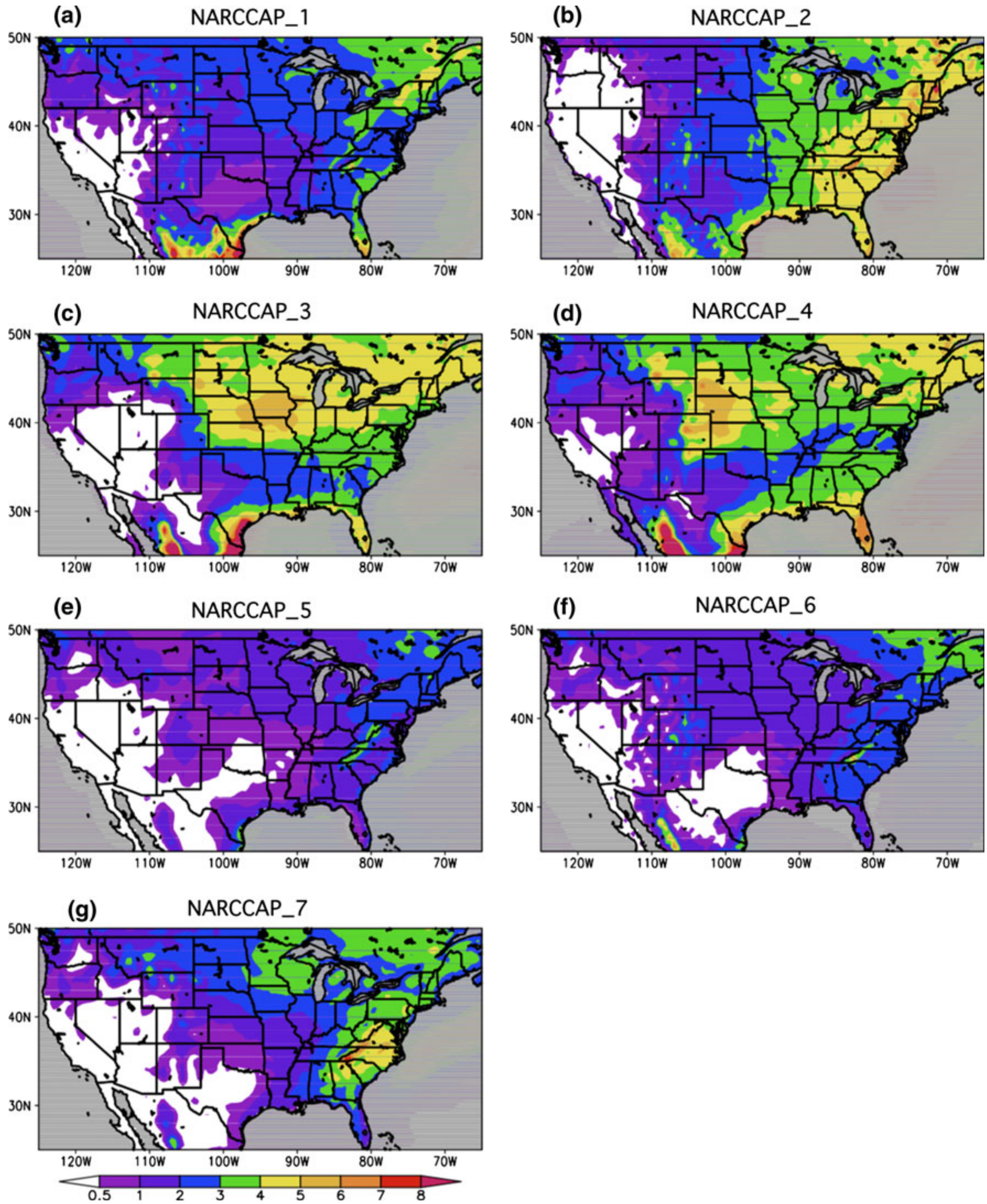

Fig. 4 Precipitation rate (mm/day) averaged July–August of 1981–2000 from the **a** NARCCAP_1, **b** NARCCAP_2, **c** NARCCAP_3, **d** NARCCAP_4, **e** NARCCAP_5, **f** NARCCAP_6, and **g** NARCCAP_7 simulations. Values over water are masked *grey*. Refer to Fig 2e for observed precipitation

the warm season only. Also, throughout this section we group the analysis by the first and second halves of the warm season, corresponding roughly to March through June and June through October respectively, to focus on periods of wetter or drier projections. (June is grouped with the first or second half of the warm season depending on the region of analysis, since the sign of predicted precipitation changes varies regionally over the central U.S. in June.).

The projected mid-twenty-first century changes are similar between the southern Great Plains and Midwest, with wetter conditions in March–May, drying in June–

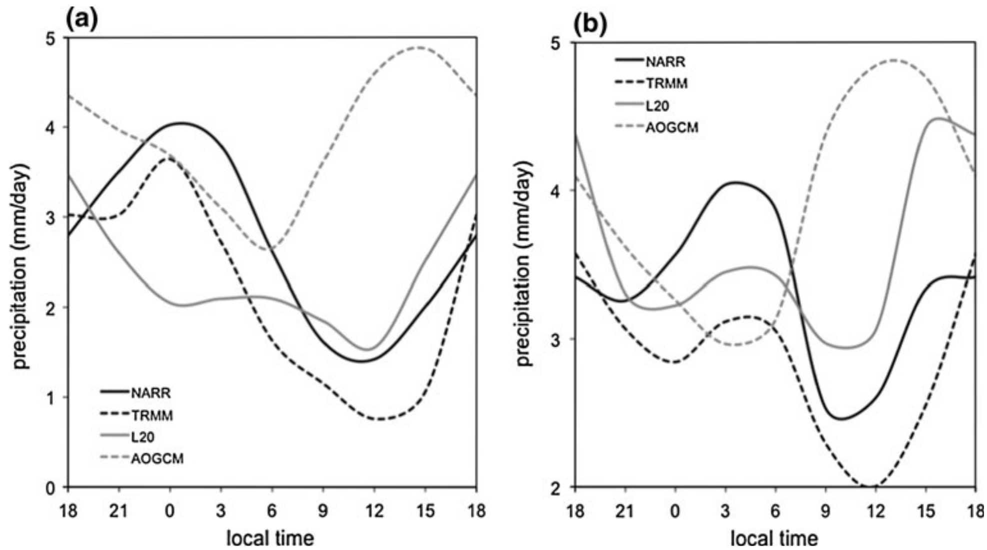

Fig. 5 The 3-hourly precipitation rate (mm/day) in June–August of 1998–2009 from TRMM (*dash black*), 1979–2007 from NARR (*solid black*), 1981–2000 from the 30 km domain of L20 (*solid grey*), and 1991–2000 from the GFDL 2.0 AOGCM (*dash grey*) averaged over the **a** northern and southern Great Plains together and **b** Midwest

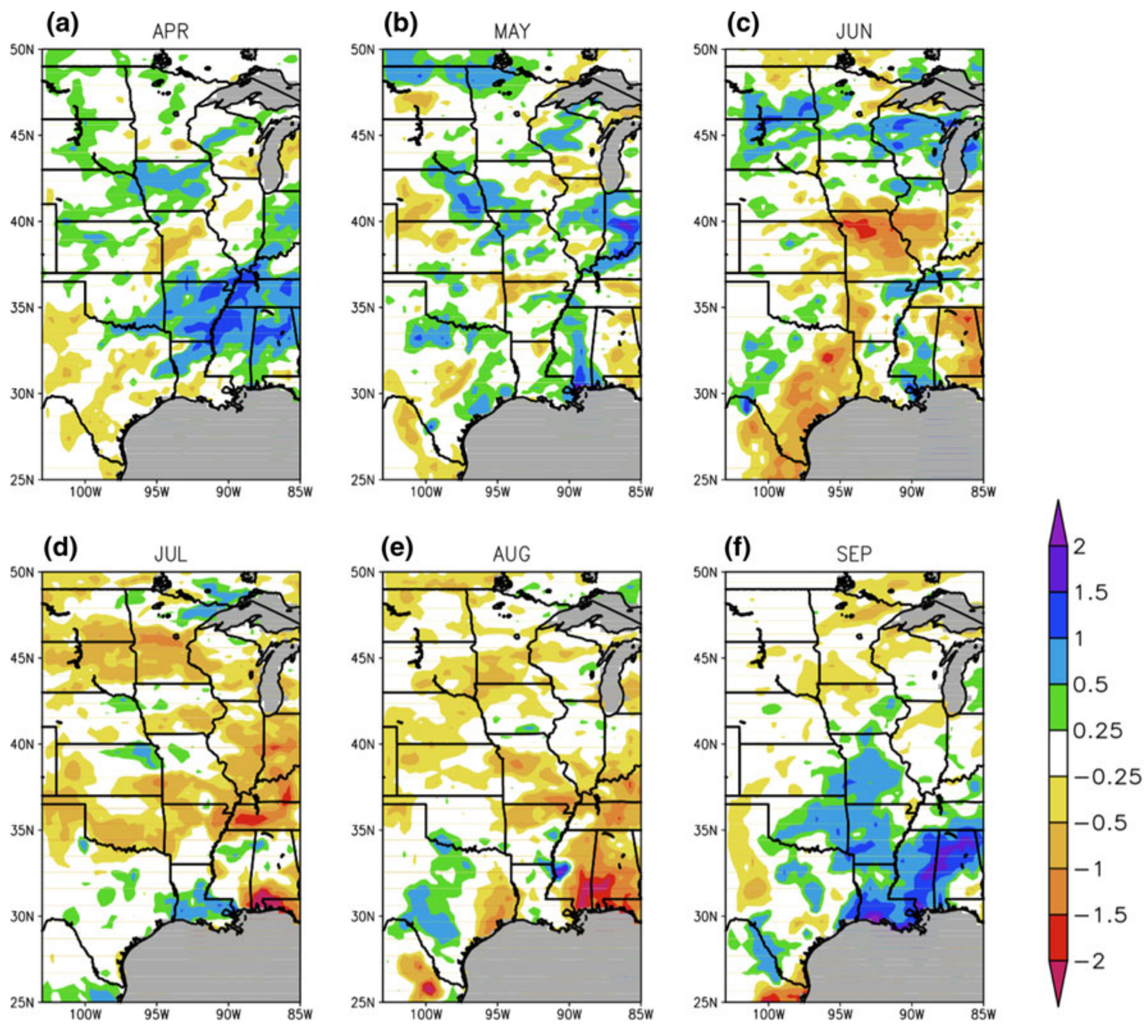

Fig. 6 Future precipitation differences (mm/day, 2041–2060 minus 1981–2000) from the 30-km domain of M21–L20 in **a** April, **b** May, **c** June, **d** July, **e** August, and **f** September. Values over water are masked *grey*

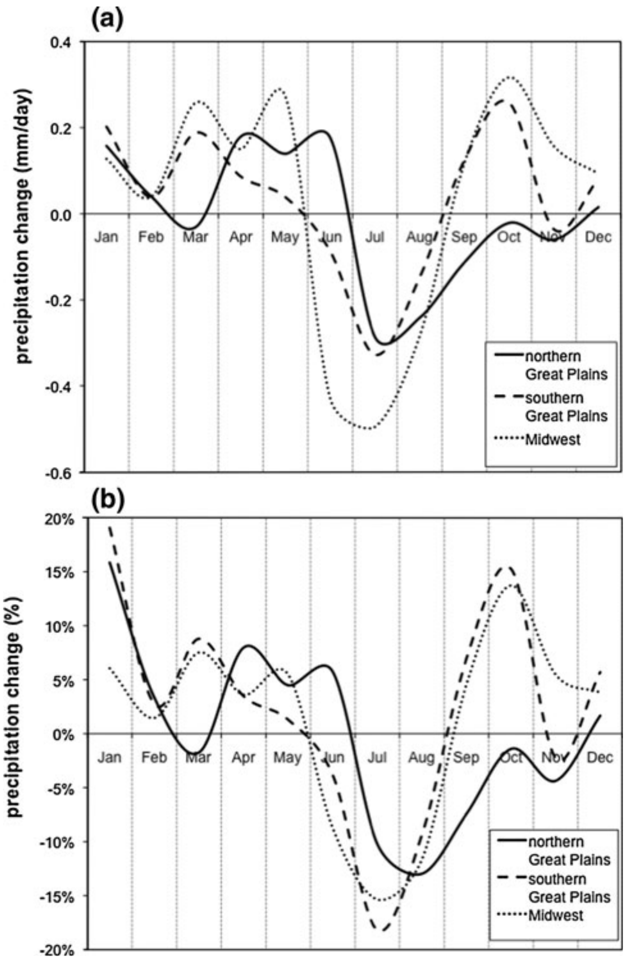

Fig. 7 Future precipitation differences (2041–2060 minus 1981–2000) from the 30-km domain of M21–L20 for the northern Great Plains (*solid*), southern Great Plains (*dash*), and Midwest (*dot*) expressed as **a** mm/day and **b** percent

August, and wetter conditions again in September–October (Fig. 7). While absolute changes (Fig. 7a) are weaker over the southern Great Plains, ranging from −0.33 to 0.25 mm/day compared to −0.5 to 0.33 mm/day in the Midwest, the percentage changes (Fig. 7b) are similar, peaking near +8 % in MAM, −15 % in JJA, and +15 % in SO over both regions. Projected monthly warm season precipitation changes over the northern Great Plains are similar in relative magnitude to those over the southern Great Plains and Midwest and are similar in absolute magnitude to those over the southern Great Plains. However, compared with the southern Great Plains and Midwest, wetter conditions are projected 1 month later, during April–June, and prolonged drier conditions are projected to begin 1 month later, during July–November, over the northern Great Plains.

The monthly climatological precipitation predictions of M21–L20 are next compared with those from the ensembles of 15 IPCC AR4 AOGCM and 7 NARCCAP RCM simulations. This is done because confidence in future climate change predictions is supported by agreement among multi-model ensembles, and because agreement between projections from the RCM that is downscaled with anomalies with those from the ensemble of AOGCMs and dynamically downscaled RCMs offers support for the downscaling with anomalies methodology. Figure 8 shows mid-twenty-first century percentage monthly precipitation changes from each of the 15 AOGCMs and the AOGCM average, each of the 7 NARCCAP RCM simulations and their average, and the M21–L20 simulation, for the northern and southern Great Plains and Midwest. To evaluate agreement among the models, we also calculate the number of models that predict wetter or drier conditions during the mid-twenty-first century (Tables 3, 4 and 5) and assign an "inconclusive," "likely," or "very likely" chance of occurrence when 33–66 %, greater than 66 %, or greater than 90 % of the ensemble members agree on the sign of the future precipitation change. This method is based on the likelihood scale of the IPCC AR4 and provides a quantifiable measure of model agreement. Note, that since the ensemble size of the AOGCMs is larger than that of the NARCCAP RCMs, a "very likely" change predicted by the AOGCMs is more significant than a "very likely" changed predicted by the NARCCAP RCMs.

There is a consensus among the multi-model ensemble predictions for wetter mid-twenty-first century conditions in March through May over the northern Great Plains, with both ensemble averages predicting wetter conditions (Fig. 8a) and the AOGCM and NARCCAP runs together predicting likely wetter conditions (Table 3). These projections are corroborated by the M21–L20 prediction of wetter conditions in April–June.

Such a consensus does not emerge during the second half of the warm season over the northern Great Plains. The ensemble mean precipitation changes of both the AOGCMs and NARCCAP RCMs are weak in June through August (Fig. 8a), and the change is inconclusive in June through August in the AOGCMs and inconclusive in June and August and likely wetter in July in the NARCCAP RCMs (Table 3). The M21–L20 predictions of drier conditions in July through September are not corroborated by the multi-model ensemble.

Over the southern Great Plains during March through May, precipitation changes projected by the AOGCM ensemble are inconclusive (Table 4) and average near zero (Fig. 8b), while the NARCCAP RCMs predict likely wetter conditions in April and May (Table 4), with the ensemble average increase of about 15 % (Fig. 8b). This offers some support of the M21–L20 projection of wetter conditions in March and April, although the timing is shifted by 1 month. On the other hand, there is a striking consensus among the multi-model projections over the southern Great

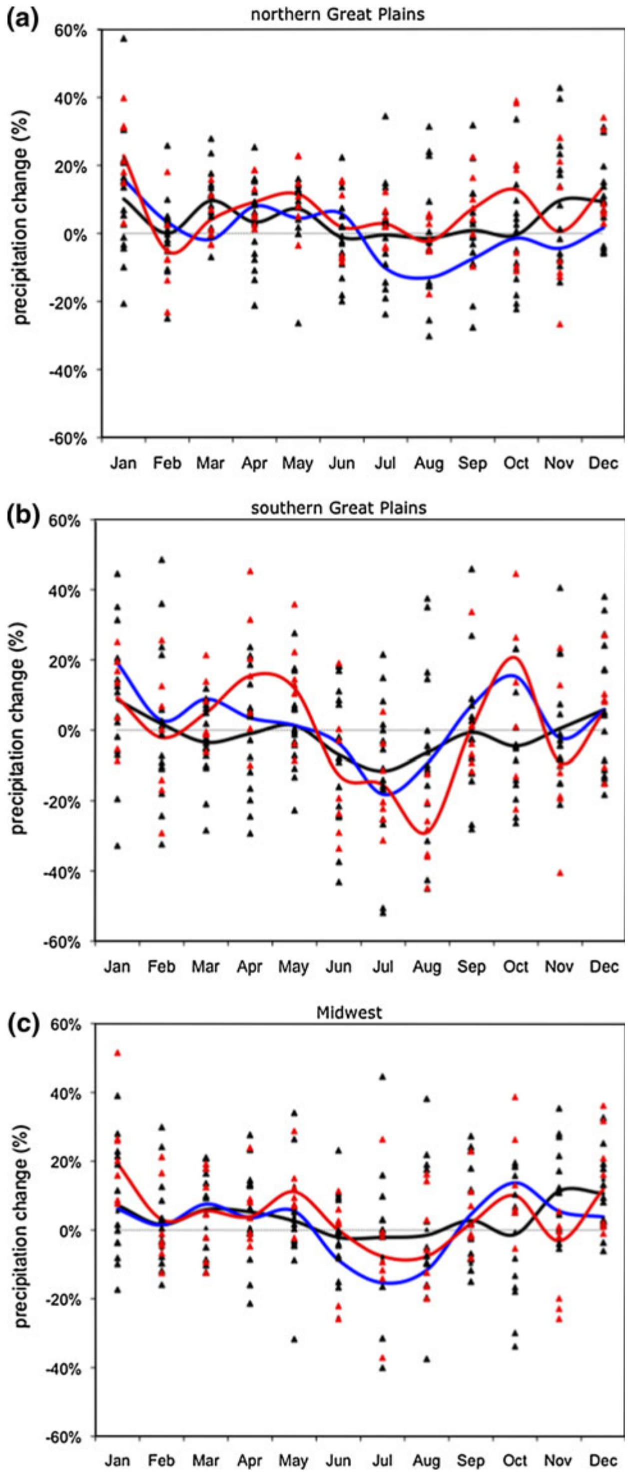

Fig. 8 Future precipitation differences (2041–2060 minus 1981–2000, percent) from the 30 km domain of M21–L20 (*blue line*), each of the 15 AOGCMs (*black marks*), the AOGCM average (*black line*), each of the 7 NARCCAP RCM simulations (*red marks*), and the average of the 7 NARCCAP RCM simulations (*red line*) averaged over the **a** northern Great Plains, **b** southern Great Plains, and **c** Midwest

Plains in the second half of the warm season, with the AOGCMs predicting likely drier conditions (Table 4) of up to −10 % in the ensemble average (Fig. 8b) in July and August and the NARCCAP RCMs predicting likely drier conditions (Table 4) reaching up to −30 % in the ensemble average (Fig. 8b) during June through August. This provides strong support of the predictions of drier conditions of up to −20 % during June through August over southern Great Plains from M21–L20 (Fig. 8b).

Over the Midwest the 15-member AOGCM ensemble predicts likely wetter conditions in March and April (Table 5) of up to 5 % (Fig. 8c), while the 7-member ensemble of NARCCAP RCMs simulates likely wetter conditions (Table 5) of up to 10 % (Fig. 8c) later, in May and June. The M21–L20 predictions of wetter conditions during March through May are in general agreement with the AOGCMs and NARCCAP RCMs. In the second half of the warm season, the AOGCMs predict likely drier conditions in June over the Midwest (Table 5), although the ensemble average is weak (Fig. 8c). The NARCCAP RCMs predict likely drier conditions (Table 5) of nearly 10 % in the ensemble average (Fig. 8c) 1 month later in July. The L21–L20 predictions of drier conditions during June through August (Fig. 8c) are again in general agreement with the NARCCAP predictions.

5.2 Extremes in daily precipitation

Changes in measures of extreme daily precipitation are assessed with the indices of the ETCCDI/CRD (Expert Team on Climate Change and Detection Indices/Climate Research Division; Karl et al. 1999; Peterson et al. 2001). The statistical software package RClimDex is used to calculate indices at every fourth latitude and longitude gridpoint on the 30-km domain of the L20 and M21 simulations. Subsampling is done for efficiency and does not negate the 30-km resolution of the original output because the physical processes that determine the response still operate on this scale. As shown below, statistically significant projected changes in measures of extreme daily precipitation and 2-m air temperature have a very limited and widespread areal coverage, respectively, which is not likely to be sensitive to the subsampling.

Climate indices for extremes in daily precipitation include the annual precipitation total when the daily precipitation rate exceeds the 95th and the 99th percentile of the control period (1981–2000), the monthly maximum of the daily precipitation rate, and the annual count of days when daily precipitation exceeds 10 mm, 20 mm, and 25 mm. Changes between L20 and M21 in all precipitation indices are statistically significant (10 % level) over only a

Table 3 Levels of agreement on monthly precipitation predictions for the mid twenty-first century over the northern Great Plains from 15 AOGCMs, 7 NARCCAP RCMs, and the 22 AOGCMs and NARCCAP RCMs together, and the percent change from M21–L20. Criteria for "inconclusive," "likely," and "very likely" correspond to 33–66 %, greater than 66 %, and greater than 90 % of the models predicting the same sign of precipitation change

	AOGCMs	NARCCAP	AOGCM and NARCCAP	M21–L20 (%)
Jan	Likely wetter	Very likely wetter	Likely wetter	15.8
Feb	Inconclusive	Likely drier	Inconclusive	3.3
Mar	Likely wetter	Inconclusive	Likely wetter	−1.8
Apr	Inconclusive	Very likely wetter	Likely wetter	8.0
May	Likely wetter	Likely wetter	Likely wetter	4.5
Jun	Inconclusive	Inconclusive	Inconclusive	5.7
Jul	Inconclusive	Likely wetter	Inconclusive	−10.2
Aug	Inconclusive	Inconclusive	Inconclusive	−13.0
Sep	Inconclusive	Likely wetter	Inconclusive	−7.4
Oct	Inconclusive	Inconclusive	Inconclusive	−1.4
Nov	Inconclusive	Inconclusive	Inconclusive	−4.4
Dec	Likely wetter	Very likely wetter	Likely wetter	1.7

Table 4 Same as Table 3, but for the southern Great Plains

	AOGCMs	NARCCAP	AOGCM and NARCCAP	M21–L20 (%)
Jan	Likely wetter	Likely wetter	Likely wetter	19.1
Feb	Inconclusive	Inconclusive	Inconclusive	2.7
Mar	Inconclusive	Inconclusive	Inconclusive	8.8
Apr	Inconclusive	Likely wetter	Inconclusive	3.5
May	Inconclusive	Likely wetter	Inconclusive	1.3
Jun	Inconclusive	Likely drier	Inconclusive	−3.8
Jul	Likely drier	Likely drier	Likely drier	−18.2
Aug	Likely drier	Very likely drier	Likely drier	−9.4
Sep	Inconclusive	Inconclusive	Inconclusive	6.9
Oct	Likely drier	Likely wetter	Inconclusive	15.3
Nov	Likely drier	Likely drier	Likely drier	−2.3
Dec	Inconclusive	Likely wetter	Inconclusive	5.7

Table 5 Same as Table 3, but for the Midwest

	AOGCMs	NARCCAP	AOGCM and NARCCAP	M21–L20 (%)
Jan	Inconclusive	Very likely wetter	Likely wetter	6.1
Feb	Inconclusive	Likely drier	Inconclusive	1.5
Mar	Likely wetter	Inconclusive	Inconclusive	7.5
Apr	Likely wetter	Inconclusive	Inconclusive	3.6
May	Inconclusive	Likely wetter	Likely wetter	5.5
Jun	Likely drier	Likely wetter	Inconclusive	−8.7
Jul	Inconclusive	Likely drier	Inconclusive	−15.4
Aug	Inconclusive	Inconclusive	Inconclusive	−11.7
Sep	Inconclusive	Inconclusive	Inconclusive	4.5
Oct	Inconclusive	Likely wetter	Inconclusive	13.7
Nov	Likely wetter	Likely drier	Inconclusive	5.5
Dec	Likely wetter	Likely wetter	Likely wetter	3.8

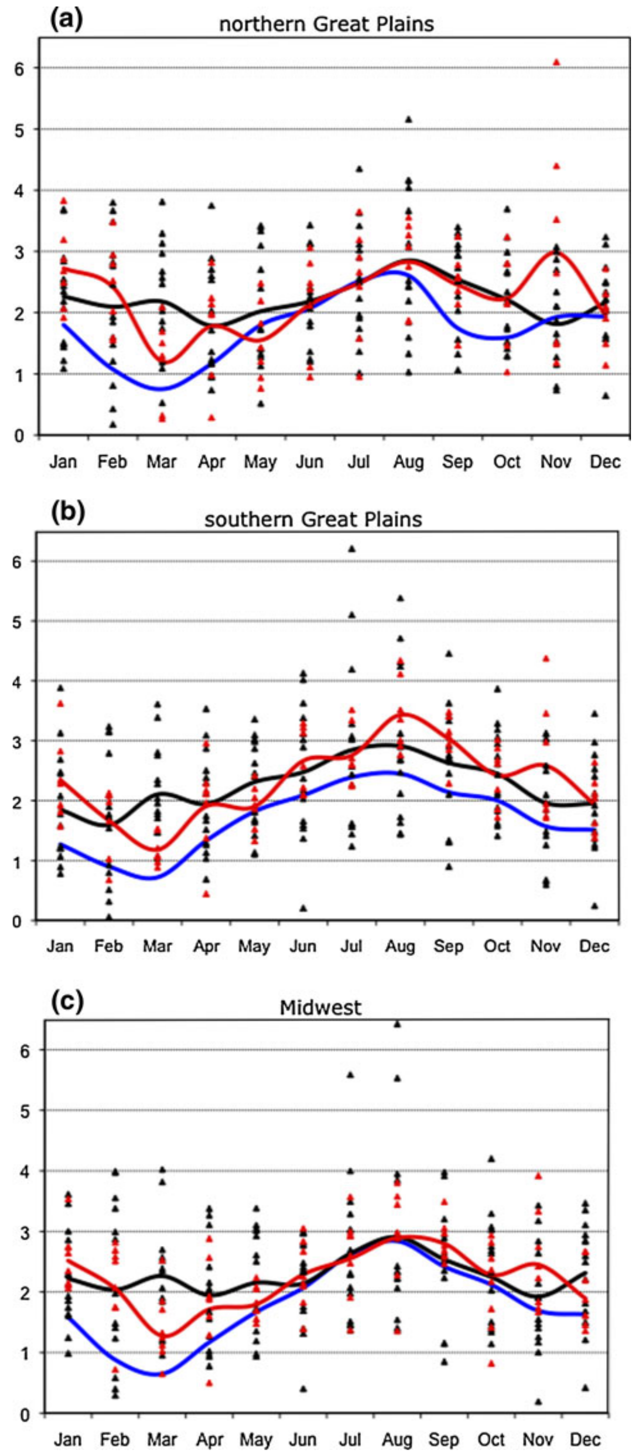

Fig. 9 Same as Fig. 8, but for 2-m air temperature (K). **a** Northern Great Plains, **b** southern Great Plains, and **c** Midwest

limited portion of the Great Plains and Midwest and are not very regionally coherent. It is possible that more widespread changes in these measures of extreme precipitation would be apparent towards the late twenty-first century, as suggested by the increase in intensity and frequency of extreme 6-hourly precipitation events predicted by regional downscaling simulations using WRF with boundary conditions from the Community Climate System Model (Bukovsky and Karoly 2011).

Fig. 10 Changes in extreme climate indices between M21 and L20 ▶ (*shaded*), with insignificant changes at the 10 % level masked grey. The change in **a** monthly maximum of the daily maximum temperature (K/50 year), **b** monthly maximum of the daily minimum temperature (K/50 year), **c** monthly minimum of the daily maximum temperature (K/50 year), **d** monthly minimum of the daily minimum temperature (K/50 year), **e** ice days (week/50 year), **f** frost days (week/50 year), **g** growing season (week/50 year), **h** summer days (week/50 year), **i** tropical nights (week/50 year), **j** warm days (week/50 year), **k** warm nights (week/50 year), **l** cool days (week/50 year), **m** cool nights (week/50 year), **n** warm spell duration (week/50 year), and **o** cold spell duration (days/50 year). Indices are not calculated over white regions

5.3 Monthly mean 2-m air temperature

Projected mid-twenty-first century changes in monthly mean 2-m air temperature from the M21–L20, 15 AOGCM, and 7 NARCCAP RCM simulations are shown in Fig. 9. There is a large spread among individual ensemble members, up to 5 K, but overall the predicted magnitude and seasonal changes in 2-m air temperature are more consistent across model type and region than for precipitation. The AOGCM ensemble average, NARCCAP RCM ensemble average, and M21–L20 each produce a maximum increase in 2-m air temperature in August over the northern Great Plains (2.9, 2.8, and 2.6 K, respectively; Fig. 9a), southern Great Plains (2.9, 2.4, and 2.5 K, respectively; Fig. 9b), and Midwest (2.9, 2.9, and 2.8 K, respectively; Fig. 9c). The smallest change in monthly mean 2-m air temperature projected by M21–L20 and the NARCCAP average is simulated in March over the northern and southern Great Plains and Midwest and ranges from 0.7 to 1.3 K (Fig. 9). In the AOGCM average, the smallest increase in monthly mean 2-m air temperature occurs in April over the northern Great Plains and Midwest and in February over the southern Great Plains, and is warmer than that predicted by the RCMs, ranging from 1.6 to 2 K (Fig. 9). The projected area-average increase in 2-m temperature in M21–L20 is significant (10 % level; one-tailed t-tests) in March over the northern and southern Great Plains and in August over all three regions.

The monthly 2-m temperature is projected to warm year round over the northern and southern Great Plains and Midwest in the AOGCM and NARCCAP RCM averages and M21–L20, with an annual projected increase of 2.2–2.3 K in the AOGCM average, 2.2–2.3 K in the NARCCAP average, and 1.7–1.8 K in M21–L20.

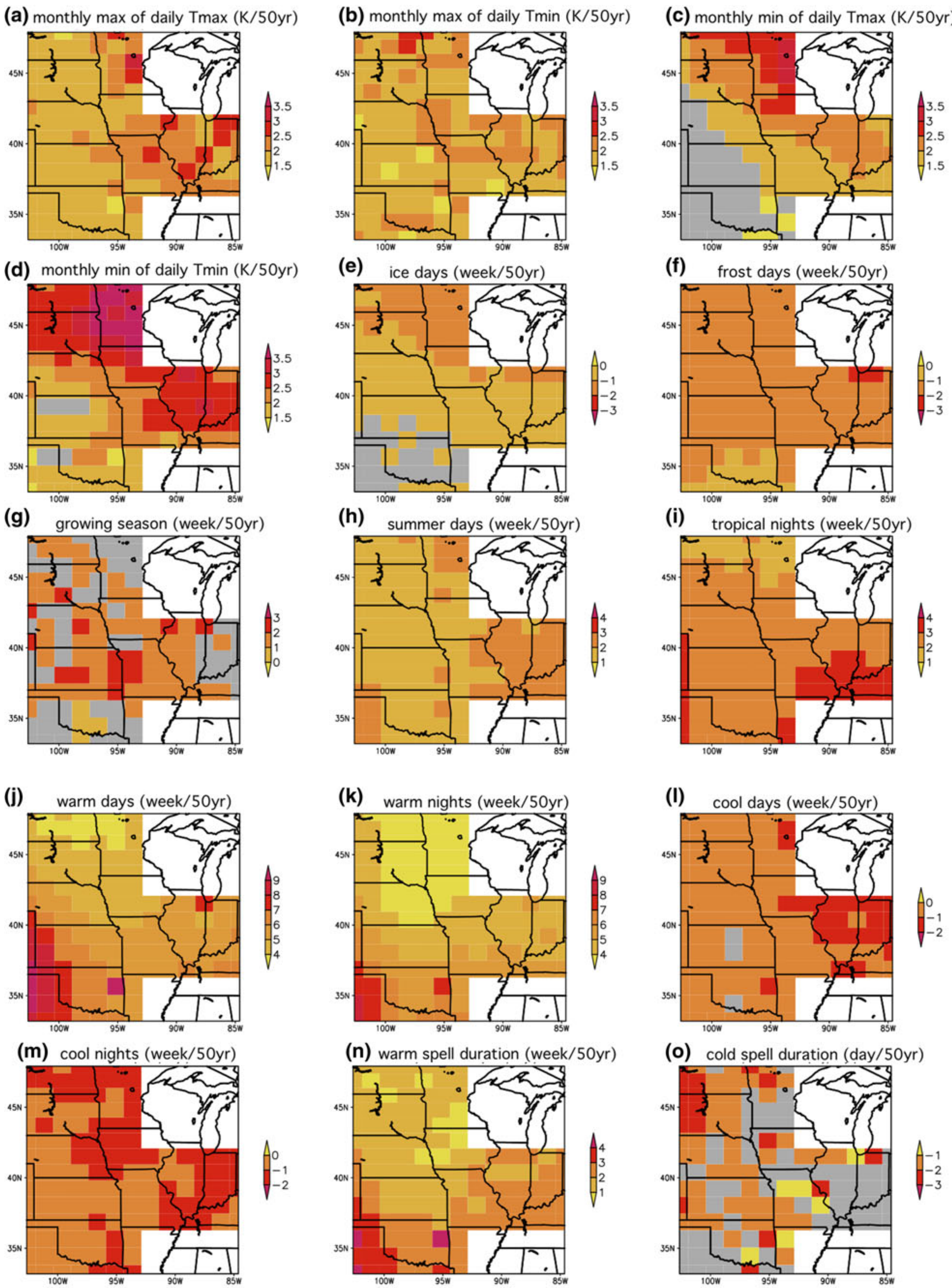
(a) monthly max of daily Tmax (K/50yr)
(b) monthly max of daily Tmin (K/50yr)
(c) monthly min of daily Tmax (K/50yr)
(d) monthly min of daily Tmin (K/50yr)
(e) ice days (week/50yr)
(f) frost days (week/50yr)
(g) growing season (week/50yr)
(h) summer days (week/50yr)
(i) tropical nights (week/50yr)
(j) warm days (week/50yr)
(k) warm nights (week/50yr)
(l) cool days (week/50yr)
(m) cool nights (week/50yr)
(n) warm spell duration (week/50yr)
(o) cold spell duration (day/50yr)

5.4 Extremes in daily 2-m air temperature

The ETCCDI/CRD indices are used to assess changes in extremes in daily 2-m air temperature including

- monthly maximum and minimum of daily maximum and minimum temperature
- number of ice (frost) days—annual count of days when the daily maximum (minimum) is less than 0 °C
- growing season length—annual count between the first span of at least 6 days when the temperature exceeds 5 °C and the first span after July 1 of 6 days when the temperature is less than 5 °C
- number of summer days (tropical nights)—annual count of days when the daily maximum exceeds 25 °C (minimum exceeds 20 °C)
- warm days (nights)—number of days (nights) when the daily maximum (minimum) temperature exceeds the 90th percentile of the control period
- cool days (nights)—number of days (nights) when the daily maximum (minimum) temperature is less than the 10th percentile of the control period
- warm (cold) spell duration—annual count of days with at least 6 consecutive days when the daily maximum temperature exceeds the 90th percentile (minimum temperature is less than the 10th percentile) of the control period

Figure 10 shows statistically significant (10 % level; one-tailed t-tests) changes between L20 and M21 in these indices, which exhibit more widespread statistical significance compared to the precipitation indices. The monthly maximum of the daily maximum temperature (Fig. 10a) and monthly maximum of the daily minimum temperature (Fig. 10b) are both projected to increase by 1.5–2 K over the northern and southern Great Plains and are projected to increase by 2–3 K and 1.5–2.5 K, respectively, over the Midwest. The projected increase in the monthly minimum of the daily maximum temperature (Fig. 10c), 2.5–3.5 K, exceeds that of the monthly maximum of the daily maximum temperature (Fig. 10a) over the northern Great Plains. Similarly, the projected warming of the monthly minimum of the daily minimum temperature (Fig. 10d), which reaches up to 3.5 K, is greater than that of the monthly maximum of the daily minimum (Fig. 10b) over both the northern Great Plains and Midwest.

Indices based on the number of days a temperature threshold is reached are useful to quantify changes in season length. M21 and L20 project an annual reduction in the number of ice days by up to 2 weeks (Fig. 10e) and frost days by 1–2 weeks (Fig. 10f) over most of the Great Pains and Midwest. In addition, a 1–3 week lengthening of the temperature-based growing season is projected for the mid-twenty-first century over much of the Great Plains and Midwest (Fig. 10g). Similarly, the projected number of summer days (Fig. 10h) increases by 1–3 weeks, and the number of tropical nights (Fig. 10i) increases by 1–3 weeks over the Great Plains and 2–4 weeks over the Midwest. These changes suggest a lengthening of the warm season by 1–4 weeks at the expense of a 1–2 week cold season reduction.

Changes in the warm and cool days and nights provide information about the frequency of extreme daily 2-m air temperature events, since these indices are based on the 10th and 90th percentiles. There is 4–5 week increase in the number of warm days (Fig. 10j) and warm nights (Fig. 10k) projected over the northern Great Plains, with larger increases of 5–7 weeks over the Midwest and 6–9 weeks over the southern Great Plains. The projected decrease in the number of cool days (Fig. 10l) and cool nights (Fig. 10m) is up to 2 weeks. This unequal shift in the warm and cool tails of the daily 2-m temperature distribution, with a relatively small changes in the cool tail between the late twentieth century and the mid-twenty-first century, suggests an increase in the variability of daily extreme temperatures. The warm spell duration (Fig. 10n) is projected to lengthen by 1–4 weeks, indicating more frequent and longer occurrences of heat waves, while the cold spell duration (Fig. 10o) is projected to shorten by only 1–3 days. The projected changes in warm and cold spell duration also reflect the unequal shift in the cool and warm tails of the 2-m air temperature distribution.

6 Conclusions

A regional climate model (RCM) is used to generate climate projections at 30-km resolution for the mid-twenty-first century over the central U.S., and results are compared with projections from 15 AOGCMs from the IPCC AR4 and 7 RCM simulations from the NARCCAP to identify consistent climate change signals. In an effort to produce the most informed future predictions possible, we perform an intercomparison of these three methodologies, with an understanding of the advantages and disadvantages of each.

The regional model simulation design, referred to as "downscaling with anomalies," differs from the dynamic downscaling method which prescribes lateral boundary conditions and SST to a RCM directly from AOGCMs for both the control and future integrations, potentially introducing AOGCM biases into the RCM simulations. Here, lateral boundary conditions and SST for the control are obtained from reanalysis to reduce model bias, and boundary conditions for the future are created by adding anomalies from AOGCMs to the reanalysis. This method accounts for changes in the mean state of the boundary conditions, but the interannual variability and transients prescribed on the lateral boundaries remain the same between the control and future simulations. (Transients generated within the RCM domain are different.).

There is strong agreement among the ensembles of AOGCMs and NARCCAP RCMs and the RCM downscaled with anomalies in projecting wetter mid- twenty-first century conditions (about 10 %) over the northern Great Plains during April and May, while the NARCCAP RCMs and the RCM downscaled with anomalies project wetter conditions (up to 15 %) in the southern Great Plains in April. During June through August a strong multi-model consensus predicts drier conditions (−10 to −30 %) over the southern Great Plains, while the NARCCAP RCMs and the RCM downscaled with anomalies produce drier conditions (−10 to −15 %) over the Midwest in July. However, precipitation predictions over the northern Great Plains are inconclusive in June through August when there is no consensus among the models. Strong agreement among the AOGCMs, NARCCAP RCMs, and the RCM downscaled with anomalies supports confidence in the future predictions; to further our understanding of the future predictions of the RCM downscaled with anomalies, connections between precipitation and circulation changes, including the Great Plains low-level jet, are analyzed in Part II (Patricola and Cook 2012). Changes in measures of extremes in daily precipitation projected by the RCM downscaled with anomalies are assessed with indices of the ETCCDI/CRD. Statistically significant mid-twenty-first century changes are projected over only a limited area of the central U.S. for all measures of extremes in daily precipitation.

Projected changes in mid-twenty-first century monthly mean 2-m air temperature are very consistent across model type, with the AOGCM ensemble average, NARCCAP RCM ensemble average, and RCM downscaled with anomalies producing a maximum increase in 2-m air temperature in August of 2.6–2.9 K over the northern Great Plains, 2.4–2.9 K over the southern Great Plains, and 2.8–2.9 K over the Midwest.

Changes in extremes in daily 2-m air temperature from the RCM downscaled with anomalies are statistically significant over widespread regions of the central U.S. While the annual number of days during which the daily maximum temperature exceeds the 90th percentile of the late-twentieth century is projected to increase by 4–9 weeks in the mid-twenty-first century, the number of annual days during which the daily maximum temperature is below the 10th percentile of the late-twentieth century simulation is projected to decrease by up to 2 weeks. Similarly, the warm spell duration is expected to lengthen by 1–4 weeks, while the cold spell duration is shortened by only 1–3 days in the mid-twenty-first century projections, indicating an unequal shift in the cool and warm tails of the daily 2-m temperature distribution.

Comparison of monthly mid-twenty-first century precipitation and 2-m air temperature predictions from the RCM downscaled with anomalies with the ensembles of AOGCM and NARCCAP RCM simulations shows a promising level of coherence. This multi-model coherence suggests that in this case, the credibility of the future projections may not be significantly reduced by climate bias in the ensemble of AOGCMs, climate bias introduced into the ensemble of dynamically downscaled RCMs by using model output as boundary conditions, and using only mean-state future anomalies in the boundary conditions of the RCM downscaled with anomalies. For the RCM downscaled with anomalies, this also suggests that prescribing changes in greenhouse gas concentrations and mean-state changes in SST and lateral boundary conditions may be sufficient to project mean-state changes in a warming scenario. While the downscaling with anomalies methodology produces future monthly mean precipitation and 2-m air temperature projections that generally compare well with those from an ensemble of AOGCMs and dynamically downscaled RCMs, we note that this relatively new methodology warrants additional testing and would not be appropriate to assess changes in interannual variability.

Acknowledgments This research was supported in part by the Department of Energy BER Program, and simulations were run on the Texas Advanced Computing Center (TACC). Output from the IPCC AR4 AOGCM simulations is maintained by the Program for Climate Model Diagnosis and Intercomparison. We wish to thank the North American Regional Climate Change Assessment Program (NARCCAP) for providing the data used in this paper. NARCCAP is funded by the National Science Foundation (NSF), the U.S. Department of Energy (DoE), the National Oceanic and Atmospheric Administration (NOAA), and the U.S. Environmental Protection Agency Office of Research and Development (EPA). RClimDex is developed and maintained by Xuebin Zhang and Yang Feng at the Climate Research Division of the Meteorological Service of Canada. We would also like to thank Drs. E. K Vizy, B. Pu, P. Hess, S. Colucci, three anonymous reviewers, and Dr. E. K. Schneider for their helpful comments which have helped improve this work.

References

Arritt RW, Rummukainen M (2011) Challenges in regional-scale climate modeling. Bull Am Meteorol Soc 92:365–368

Bah A (1987) Towards the prediction of Sahelian rainfall from sea surface temperatures in the Gulf of Guinea. Tellus 39A:39–48

Bukovsky MS, Karoly JD (2011) A regional modeling study of climate change impacts on warm-season precipitation in the Central United States. J Clim 24:1985–2002

Carbone RE, Tuttle JD (2008) Rainfall occurrence in the U.S. warm season: the diurnal cycle. J Clim 21:4132–4146

Chen H, Zhou T, Yu R, Li J (2009) Short Communication: Summer rain fall duration and its diurnal cycle over the US Great Plains. Int J Climatol 29:1515–1519

Cook KH, Vizy EK (2008) Effects of twenty-first-century climate change on the Amazon rain forest. J Clim 21:542–560
Cook KH, Vizy EK, Launer ZS, Patricola CM (2008) Springtime intensification of the Great Plains low-level jet and Midwest precipitation in GCM simulations of the twenty-first century. J Clim 21:6321–6340
Davey KM et al (2002) STOIC: A study of coupled model climatology and variability in tropical ocean regions. Clim Dyn 18:403–420
De Elía R et al (2008) Evaluation of uncertainties in the CRCM-simulated North American climate. Clim Dyn 30:113–132
Diaconescu EP, Laprise R, Sushama L (2007) The impact of lateral boundary data errors on the simulated climate of a nested regional climate model. Clim Dyn 28:333–350
Dimitrijevic M, Laprise R (2005) Validation of the nesting technique in a regional climate model and sensitivity tests to the resolution of the lateral boundary conditions during summer. Clim Dyn 25:555–580
European Centre for Medium-Range Weather Forecasts (2002) The ERA-40 archive. Reading, ECMWF: 40
Giorgi F, Bi X (2000) A study of internal variability of a regional climate model. J Geophys Res 105:29503–29521
Gong W, Wang W-C (2000) A regional model simulation of the 1991 severe precipitation event over the Yangtze–Huai river Valley, Part II: model bias. J Clim 13:93–108
Han J, Roads JO (2004) U.S. climate sensitivity simulated with the NCEP regional spectral model. Clim Chang 62:115–154
Huffman GJ, Adler RF, Bolvin DT, Gu G, Nelkin EJ, Bowman KP, Hong Y, Stocker EF, Wolff DB (2007) The TRMM Multi-satellite precipitation analysis: quasi-global, multi-year, combined-sensor precipitation estimates at fine scale. J Hydrometeor 8:38–55
IPCC (2000) Emissions scenarios. In: Nakicenovic N, Swart R (eds) Cambridge University Press, Cambridge, UK, 570 pp
IPCC (2007) Climate change 2007: the physical science basis. In: Solomon S, Qin D, Manning M, Chen Z, Marquis M, Averyt KB, Tignor, Miller HL (eds) Contribution of Working Group I to the fourth assessment report of the intergovernmental panel on climate change. Cambridge University Press, Cambridge, United Kingdom and New York, NY, USA, 996 pp
Kalnay E et al (1996) The NCEP/NCAR 40-year reanalysis project. Bull Am Meteorol Soc 77:437–471
Kanamitsu M, Ebisuzaki W, Woollen J, Yang S-K, Hnilo JJ, Fiorino M, Potter GL (2002) NCEP-DOE AMIP-II reanalysis (R-2). Bull Am Meteorol Soc 83:1631–1643
Karl TR, Nicholls N, Ghazi A (1999) CLIVAR/GCOS/WMO workshop on indices and indicators for climate extremes: workshop summary. Clim Chang 42:3–7
Kunkel KE, Angel JR (1989) Perspective on the 1988 Midwestern drought. EOS 70:817–819
Lamb PJ (1978) Case studies of tropical Atlantic surface circulation patterns during recent sub-Saharan weather anomalies: 1967 and 1968. Mon Wea Rev 106:482–491
Lee M-I, Schubert SD, Suarez MJ, Held IM, Lau N-C, Ploshay JJ, Kumar A, Kim H-K, Schemm J-KE (2007) An analysis of the warm-season diurnal cycle over the continental United States and northern Mexico in general circulation models. J Hydrometeor 8:344–366
Lee M-I, Schubert SD, Suarez MJ, Schemm J-KE, Pan H-L, Han J, Yoo S-H (2008) Role of convection triggers in the simulation of the diurnal cycle of precipitation over the United States Great Plains in a general circulation model. J Geophys Res 113: D02111. doi:10.1029/2007JD008984
Liang X-Z, Li L, Dai A, Kunkel KE (2004) Regional climate model simulation of summer precipitation diurnal cycle over the United States. Geophys Res Lett 31:L24208. doi:10.1029/2004GL021054
Liang X-Z, Pan J, Zhu J, Kunkel KE, Wang JXL, Dai A (2006) Regional climate model downscaling of the U.S. summer climate and future change. J Geophys Res 111:D10108. doi:10.1029/2005JD006685
Liang X-Z, Kunkel KE, Meehl GA, Jones RG, Wang JXL (2008) Regional climate models downscaling analysis of general circulation models present climate biases propagation into future projections. Geophys Res Lett 35:L08709. doi:10.1029/2007GL032849
Lott N, Ross T (2006) Tracking and evaluating U.S. billion dollar weather disasters, 1980–2005. AMS Forum: Environmental Risk and Impacts on Society: Successes and Challenges
Mearns LO, Gutowski WJ, Jones R, Leung L-Y, McGinnis S, Nunes AMB, Qian Y (2009) A regional climate change assessment program for North America. EOS 90(36):311–312
Meehl GA, Covey C, Delworth T, Latif M, Mcavaney B, Mitchell JFB, Stouffer RJ, Taylor KE (2007) The WCRP CMIP3 multimodel dataset: a new era in climate change research. Bull Am Meteorol Soc 88:1383–1394. doi:10.1175/BAMS-88-9-1383
Mesinger F et al (2006) North American regional reanalysis. Bull Am Meteorol Soc 87:343–360
Miguez-Macho G, Stenchikov GL, Robock A (2004) Spectral nudging to eliminate the effects of domain position and geometry in regional climate model simulations. J Geophys Res 109:D13104. doi:10.1029/2003JD004495
Mo KC, Paegle JN, Higgins RW (1997) Atmospheric processes associated with summer floods and droughts in the Central United States. J Clim 10:3028–3046
Patricola CM, Cook KH (2010) Northern African climate at the end of the 21st century: integrated application of regional and global climate models. Clim Dyn 35:193–212
Patricola CM, Cook KH (2012) Mid-twenty-first century climate change in the Central United States. Part II: Climate change processes. Clim Dyn. doi:10.1007/s00382-012-1379-z
Peterson TC et al (2001) Report on the Activities of the Working Group on climate change detection and related rapporteurs 1998–2001. WMO, Rep. WCDMP-47, WMO-TD 1071, Geneve, Switzerland, 143 pp
Richter I, Xie S-P (2008) On the origin of equatorial Atlantic biases in coupled general circulation models. Clim Dyn 31:587–598
Schneider EK, Fennessy MJ, Kinter JL (2009) A statistical–dynamical estimate of winter ENSO teleconnections in a future climate. J Clim 22:6624–6638. doi:10.1175/2009JCLI3147.1
Skamarock WC et al (2008) A description of the advanced research WRF version 3. NCAR Tech. Note, NCAR/TN-475 + STR, 113 pp
Vizy EK, Cook KH (2001) Mechanisms by Which Gulf of Guinea and Eastern North Atlantic Sea surface temperature anomalies can Influence African rainfall. J Clim 14:795–821
Vukicevic T, Errico RM (1990) The influence of artificial and physical factors upon predictability estimates using a complex limited-area model. Mon Weather Rev 118:1460–1482
Weaver SJ, Nigam S (2008) Variability of the Great Plains low-level jet: large-scale circulation context and hydroclimate impacts. J Clim 21:1532–1551
Yang H, Wang B, Wang B (2011) Reducing biases in regional climate downscaling by applying Bayesian model averaging on large-scale forcing. Clim Dyn. doi:10.1007/s00382-011-1260-5